



# Mg-doped $\text{Al}_{0.85}\text{Ga}_{0.15}\text{N}$ layers grown by *hot-wall* MOCVD with low resistivity at room temperature

A. Kakanakova-Georgieva<sup>\*1</sup>, D. Nilsson<sup>1</sup>, M. Stattin<sup>2</sup>, U. Forsberg<sup>1</sup>, Å. Haglund<sup>2</sup>, A. Larsson<sup>2</sup>, and E. Janzén<sup>1</sup>

<sup>1</sup> Department of Physics, Chemistry and Biology (IFM), Linköping University, 581 83 Linköping, Sweden

<sup>2</sup> Photonics Laboratory, Department of Microtechnology and Nanoscience, Chalmers University of Technology, 412 96 Göteborg, Sweden

Received 6 July 2010, revised 26 August 2010, accepted 27 August 2010  
Published online 2 September 2010

**Keywords** MOCVD, epitaxy, high-Al-content AlGa<sub>x</sub>N, p-type semiconductors, electrical properties

\* Corresponding author: e-mail anelia@ifm.liu.se, Phone: +46 13 282649

We report on the *hot-wall* MOCVD growth of Mg-doped  $\text{Al}_x\text{Ga}_{1-x}\text{N}$  layers with an Al content as high as  $x \sim 0.85$ . After subjecting the layers to post-growth in-situ annealing in nitrogen in the growth reactor, a room temperature resistivity of 7 k $\Omega$  cm was obtained, indicating an enhanced p-type conductivity compared to published data for  $\text{Al}_x\text{Ga}_{1-x}\text{N}$  layers with a lower Al content of  $x \sim 0.70$  and a room temperature resistivity of about 10 k $\Omega$  cm. It is believed that the enhanced p-type conductivity is a result of reduced compensation by native defects through growth conditions enabled by the distinct *hot-wall* MOCVD system.

The achievement of p-type Mg-doped high-Al-content  $\text{Al}_x\text{Ga}_{1-x}\text{N}$  alloys ( $x > 0.60$ ) with low resistivity at room temperature is of acknowledged importance for establishing this particular alloy system as the primary material for the development of efficient deep-UV light emitting devices. Such devices are desired for water/air purification and sterilization to name just a few of the anticipated areas of applications [1].

Difficulties in p-type doping of high-Al-content  $\text{Al}_x\text{Ga}_{1-x}\text{N}$  alloys arise because of the large thermal ionization energy of the common Mg acceptor in wide band gap  $\text{Al}_x\text{Ga}_{1-x}\text{N}$ , which is proposed to increase with increasing  $x$  [2], and the generation of compensating defects such as nitrogen vacancies during epitaxial growth, with the formation energy of such vacancies being low in high-Al-content  $\text{Al}_x\text{Ga}_{1-x}\text{N}$  [3]. Post-growth rapid thermal annealing is typically also required to activate Mg acceptors.

Since a large Mg acceptor ionization energy is predicted for  $\text{Al}_x\text{Ga}_{1-x}\text{N}$  alloys with  $x > 0.60$ , and therefore only a very small fraction (less than  $10^{-7}$ ) of the Mg acceptors contribute free holes for conduction at room temperature, conventional Hall effect and capacitance–voltage

measurements are considered unsuitable for the determination of the free hole concentration in Mg-doped high-Al-content  $\text{Al}_x\text{Ga}_{1-x}\text{N}$  [2]. Above room temperature, p-type conduction has been confirmed for Mg-doped high-Al-content  $\text{Al}_x\text{Ga}_{1-x}\text{N}$  alloys with  $x \sim 0.70$  by measuring resistivity, e.g. 40  $\Omega$  cm at 800 K for layers grown on sapphire substrates [4] and 10  $\Omega$  cm at 670 K for layers grown on SiC substrates [5]. The resistivity at room temperature for Mg-doped high-Al-content  $\text{Al}_x\text{Ga}_{1-x}\text{N}$  alloys with  $x \sim 0.70$  can be as high as  $\sim 10$  k $\Omega$  cm [4]. Despite the semiconducting character of such Mg-doped  $\text{Al}_{0.70}\text{Ga}_{0.30}\text{N}$  layers at room temperature, they could still perform as efficient p-transport layers in deep-UV light-emitting diodes, as a very thin layer (<10 nm) is needed [4].

In this Letter we report a room temperature resistivity of 7 k $\Omega$  cm for Mg-doped  $\text{Al}_x\text{Ga}_{1-x}\text{N}$  layers with an Al content as high as  $x \sim 0.85$  grown by *hot-wall* MOCVD [6] and subjected to a post-growth in-situ annealing in nitrogen in the growth reactor.

The *hot-wall* MOCVD system is based on the RF induction heating and implements TMAI/TMGa/NH<sub>3</sub> precursors delivered in a mixture of H<sub>2</sub> and N<sub>2</sub> gases [6].

The growth of  $\text{Al}_{0.85}\text{Ga}_{0.15}\text{N}$  was done at a  $\text{NH}_3$ /(TMAl + TMGa) gas-flow rate ratio of 1560. The precursor used for doping was bis(cyclopentadienyl)magnesium ( $\text{Cp}_2\text{Mg}$ ) delivered with a  $\text{Cp}_2\text{Mg}/(\text{TMAl} + \text{TMGa})$  gas-flow rate ratio of  $0.45 \times 10^{-3}$ , which determined the nominal doping level. The growth was performed on on-axis 4H-SiC substrates at a low pressure of 50 mbar. The epitaxial structure consisted of the following layer stack:  $\text{Al}_{0.85}\text{Ga}_{0.15}\text{N}:\text{Mg}/\text{Al}_{0.85}\text{Ga}_{0.15}\text{N}/\text{AlN}$  (380/385/180 nm). SIMS was employed to obtain the thickness of the individual layers in the stack, to verify the  $\text{Al}_{0.85}\text{Ga}_{0.15}\text{N}$  composition through the epitaxial structure, and to determine the dopant (Mg) and background impurity (H, C, O, and Si) concentrations [7]. With Cs primary ion bombardment, Al and Mg depth profiles were obtained using positive secondary ion detection. The instrument conditions were optimized for overall depth resolution and sensitivity. The quantification of the Al content and Mg, H, C, O, and Si concentrations was performed using the proprietary data processing method PCOR-SIMS [7]. It is vital for the doping that the Mg concentration exceeds by orders of magnitude the C, O, and Si concentrations each. An advantage of SIMS is the detection of impurities, dopants, and major elements with a single technique and irrespective of their site in the crystal lattice, and lattice distortions [8]. The latter could alter any XRD/optical spectrum, which has to be considered when correlated with SIMS results. The SIMS compositional measurements were complemented with XRD and infrared reflectivity measurements, following the instrumental conditions for both techniques as described in [9]. An Al content of  $x \sim 0.81$  was obtained by XRD, which compares well with the value obtained by SIMS. The surface morphology was studied by atomic force microscopy (AFM) in a tapping mode available through Veeco Dimension 3100 Scanning Probe Microscope. Circular transmission line measurements were carried out to obtain the resistivity of the Mg-doped  $\text{Al}_{0.85}\text{Ga}_{0.15}\text{N}$  layer, using Pt/Ni/Au (20/30/100 nm) metal contacts annealed for 5 min at  $500^\circ\text{C}$  in a nitrogen ambient.

Our study involves the use of a SiC substrate for the growth of high-Al-content  $\text{Al}_x\text{Ga}_{1-x}\text{N}$  layers. Besides the better, compared to the commonly used sapphire substrate, in-plane lattice constants and thermal expansion coefficients matching with AlN, the good thermal conductivity of SiC ( $3.7 \text{ W cm}^{-1} \text{ K}^{-1}$  for the 4H polytype) is essential to minimize the self-heating during operation of a light-emitting device, which otherwise leads to a reduction of the device efficiency and lifetime and a spectral shift of the emission [1]. The more efficient thermal management is anticipated to have a stronger impact on the performance of a deep-UV light-emitting diode than the internal absorption of the generated deep-UV emission by the SiC substrate. When grown on sapphire, which is transparent to UV emission, a more than  $10 \mu\text{m}$  thick AlN template layer is needed to reduce the thermal impedance of the devices because of the poor thermal conductivity of sapphire ( $0.35 \text{ W cm}^{-1} \text{ K}^{-1}$ ), which requires elaborate growth ap-

proaches to prevent formation of cracks and propagation of defects [10]. The SiC/AlN (180 nm) template used in this study is therefore expected to provide efficient heat dissipation when incorporated as part of a complete light-emitting device epitaxial structure. This assumption is supported by our previous work on AlGaIn/GaN HEMTs which showed a reduction of the operating temperature when grown by hot-wall MOCVD on a high quality AlN template layer on a SiC substrate [11].

In the present epitaxial structure, the growth of  $\text{Al}_{0.85}\text{Ga}_{0.15}\text{N}$  was initiated by first growing an AlN template layer on the SiC substrate at a high temperature of  $1200^\circ\text{C}$ . We note that the hot-wall MOCVD system can readily reach higher growth temperatures, up to  $1500\text{--}1600^\circ\text{C}$  with the RF heated susceptor package [6] providing efficient heating with less power consumption and less thermal dissipation loss. Therefore, specialized heater and growth chamber designs are not needed, which was suggested to be the case for other MOCVD systems to reach the expected high optimal temperatures for AlN growth [12, 13]. In previous work we have found that increasing the growth temperature of AlN to  $1200^\circ\text{C}$  is sufficient for achieving high crystal quality, as attested by the near band edge emission being dominant in cathodoluminescence [6].

The growth of the high-Al-content  $\text{Al}_{0.85}\text{Ga}_{0.15}\text{N}$  layer was done at a lower temperature of  $1100^\circ\text{C}$  to avoid thermal decomposition of GaN and to enable a linear control of the alloy composition via the gas-phase composition. Obviously, the lower temperature during the growth of the  $\text{Al}_{0.85}\text{Ga}_{0.15}\text{N}$  leads to an increased surface roughness compared to the rather smooth surface with atomic-sized steps characteristic for the AlN template layer grown at a higher temperature of  $1200^\circ\text{C}$  (Fig. 1).

Figure 2 shows SIMS depth profiles of Mg and H concentrations through the  $\text{Al}_{0.85}\text{Ga}_{0.15}\text{N}:\text{Mg}/\text{Al}_{0.85}\text{Ga}_{0.15}\text{N}$  layers in the epitaxial structure. While the Mg concentration level is characterized by a step-like profile consistent with the turn-on of the  $\text{Cp}_2\text{Mg}$  flow, the H concentration peaks at the  $\text{Al}_{0.85}\text{Ga}_{0.15}\text{N}:\text{Mg}/\text{Al}_{0.85}\text{Ga}_{0.15}\text{N}$  interface. The H concentration at the interface ( $\sim 1 \times 10^{19} \text{ cm}^{-3}$ ) is in the range

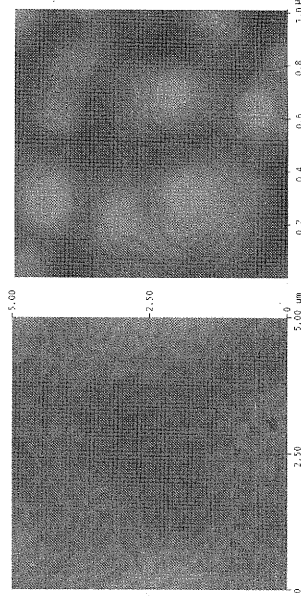


**Figure 1** (online colour at: [www.pss-rapid.com](http://www.pss-rapid.com)) AFM surface images of samples representing: (left) AlN template layer grown at a temperature of  $1200^\circ\text{C}$ ; scan size of image is  $5 \times 5 \mu\text{m}^2$ , root-mean-square roughness over the  $5 \times 5 \mu\text{m}^2$  scan is  $0.2 \text{ nm}$ , and (right) Mg-doped  $\text{Al}_{0.85}\text{Ga}_{0.15}\text{N}$  layer grown at a temperature of  $1100^\circ\text{C}$ ; scan size of image is  $1 \times 1 \mu\text{m}^2$ , root-mean-square roughness over  $10 \times 10 \mu\text{m}^2$  scan is  $1.3 \text{ nm}$ .

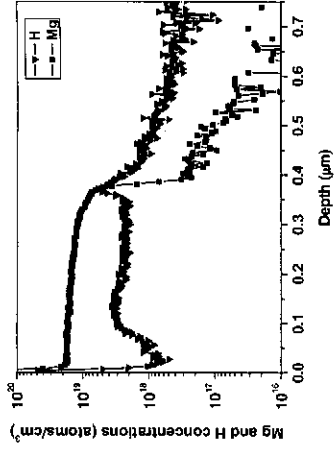


**Figure 2** (online colour at: [www.pss-rapid.com](http://www.pss-rapid.com)) SIMS depth profiles of Mg and H concentrations through the  $\text{Al}_{0.85}\text{Ga}_{0.15}\text{N}:\text{Mg}/\text{Al}_{0.85}\text{Ga}_{0.15}\text{N}$  layers in the epitaxial structure. As the zero of the depth scale matches the sample surface, concentration gradients within  $\sim 20$  nm below the sample surface are considered irrelevant.

of the Mg concentration level in the doped  $\text{Al}_{0.85}\text{Ga}_{0.15}\text{N}$  layer ( $\sim 2 \times 10^{19} \text{ cm}^{-3}$ ). The H concentration level in the  $\text{Al}_{0.85}\text{Ga}_{0.15}\text{N}:\text{Mg}$  layer is at low  $10^{18} \text{ cm}^{-3}$  and decreases to mid  $10^{17} \text{ cm}^{-3}$  in the subsurface region, thus attaining the level in the undoped  $\text{Al}_{0.85}\text{Ga}_{0.15}\text{N}$  layer. The particular H concentration profile might be related to the details of the cooling down procedure which proceeded in a mixture of  $\text{H}_2$  and  $\text{N}_2$  with ramping down the flow rate of the  $\text{H}_2$  carrier gas and obviously creating conditions for hydrogen out diffusion from the Mg-doped  $\text{Al}_{0.85}\text{Ga}_{0.15}\text{N}$  layer.

The epitaxial structure was subsequently subjected to a post-growth in-situ annealing in nitrogen in the growth reactor to cause further hydrogen out diffusion and render the Mg acceptors electrically active, which resulted in p-type conduction with a low resistivity of  $7 \text{ k}\Omega \text{ cm}$  at room temperature. This resistivity corresponds to an estimated hole concentration of  $\sim 10^{14} \text{ cm}^{-3}$ , assuming a hole mobility of  $2 \text{ cm}^2 \text{ V}^{-1} \text{ s}^{-1}$ , whereas a hole concentration in the low  $10^{13} \text{ cm}^{-3}$  has been predicted for p-type Mg doped  $\text{Al}_{0.85}\text{Ga}_{0.15}\text{N}$  with Mg acceptors at about the same optimal concentration level of  $2 \times 10^{19} \text{ cm}^{-3}$  [14].

Generally, the attainable hole concentration for a given Mg acceptor concentration is governed by compensation effects with native defects, such as nitrogen vacancies, dominating in the entire compositional range of  $\text{Al}_x\text{Ga}_{1-x}\text{N}$ ,  $0 \leq x \leq 1$  [15, 16]. It has been demonstrated that the degree of compensation can be affected by tuning the growth conditions [15, 16]. Therefore, the degree of compensation depends, at least partially, on the details of the reactor design [15]. The arrangement of the *hot-wall* MOCVD assembly in the deposition zone [6] implies reduced temperature gradients in both lateral and vertical directions, which is an essential difference compared to conventional cold-wall MOCVD systems, and thus affects the degree of thermal equilibrium over the substrate and close to the substrate surface, the genuine equilibrium process developing at the growing alloy/vapor interface and the alloy stoichiometry. Reduced temperature gradients are typically reflected in thickness, compositional and doping uniformity achieved for large area epitaxial growth, as discussed in presenting

the potential of the hot-wall MOCVD for the growth of uniform, with respect to thickness, Al composition and 2DEG properties, AlGaN/GaN-based HEMTs on 2" and 4" SiC wafers [17, 18]. Besides fundamental, and specific deposition zone related, parameters like temperature gradients, operation conditions like the  $\text{H}_2$  flow rate through the deposition zone together with the growth temperature can also influence the stoichiometry of the grown material. The  $\text{H}_2$  flow rate,  $25 \text{ l/min}$ , optimized in a previous investigation [6], and the high growth temperature of  $1100 \text{ }^\circ\text{C}$  in this case govern the dissociation of  $\text{H}_2$  at the surface and in the gas-phase, and consequently the exposition of the growing surface to atomic hydrogen. As demonstrated by first-principle calculations in the case of p-type doping of GaN by Mg, hydrogen incorporation in the material is beneficial for doping by increasing the Mg concentration and decreasing the concentration of nitrogen vacancies [19]. This effect is expected to extend to AlN, which has significantly higher hydrogen solubility than GaN, and any AlGaN alloys [3].

In summary, we reported here on the *hot-wall* MOCVD growth of Mg-doped  $\text{Al}_x\text{Ga}_{1-x}\text{N}$  layers with an Al content as high as  $x \sim 0.85$ . After subjecting the layers to post-growth in-situ annealing in nitrogen in the growth reactor, a room temperature resistivity of  $7 \text{ k}\Omega \text{ cm}$  was obtained, indicating an enhanced p-type conductivity compared to published data for  $\text{Al}_x\text{Ga}_{1-x}\text{N}$  layers with a lower Al content of  $x \sim 0.70$  and a room temperature resistivity of about  $10 \text{ k}\Omega \text{ cm}$ . The enhanced p-type conductivity is believed to be due to reduced compensation by native defects achieved by growth conditions enabled by the distinct *hot-wall* MOCVD system.

**Acknowledgements** The Swedish Foundation for Strategic Research (SSF) and The Swedish Research Council (VR) are gratefully acknowledged.

## References

- [1] A. Khan et al., *Nature Photonics* **2**, 77 (2008).
- [2] P. K. Chu et al., *Appl. Phys. Lett.* **83**, 878 (2003).
- [3] C. G. Van de Walle et al., *Appl. Phys.* **95**, 3851 (2004).
- [4] M. L. Nakarmi et al., *Appl. Phys. Lett.* **86**, 092108 (2005).
- [5] A. Chakraborty et al., *J. Appl. Phys.* **101**, 053717 (2007).
- [6] A. Kakanakova-Georgieva et al., *Cryst. Growth Des.* **9**, 880 (2009).
- [7] Evans Analytical Group® (EAG), <http://www.eaglabs.com>.
- [8] P. K. Chu et al., *J. Vac. Sci. Technol. B* **16**, 197 (1998).
- [9] A. Henry et al., *Phys. Status Solidi RRL* **3**, 145 (2009).
- [10] Q. Fareed et al., *Jpn. J. Appl. Phys.* **46**, L752 (2007).
- [11] G. J. Riedel et al., *IEEE Electron Device Lett.* **30**, 103 (2009).
- [12] Z. Chen et al., *Appl. Phys. Lett.* **93**, 191906 (2008).
- [13] K. Nagamatsu et al., *J. Cryst. Growth* **310**, 2326 (2008).
- [14] H. Amano et al., *Proc. SPIE* **7216**, 72161B (2009).
- [15] P. Kozodoy et al., *J. Appl. Phys.* **87**, 1832 (2000).
- [16] M. L. Nakarmi et al., *Appl. Phys. Lett.* **94**, 091903 (2009).
- [17] A. Kakanakova-Georgieva et al., *J. Cryst. Growth* **300**, 100 (2007).
- [18] U. Forsberg et al., *J. Cryst. Growth* **311**, 3007 (2009).
- [19] J. Neugebauer et al., *Appl. Phys. Lett.* **68**, 1829 (1996).